22nd IMEKO TC4 International Symposium & 20th International Workshop on ADC Modelling and Testing
SUPPORTING WORLD DEVELOPMENT THROUGH ELECTRICAL&ELECTRONIC MEASUREMENTS
IASI, ROMANIA, September 14-15, 2017

Ultrasound image Uniformity Assessment by Means of Sparse Matrices: Algorithm Implementation and First Results

L. Schinaia[1], A. Scorza[1], F. Orsini[1], S. A. Sciuto[1]

[1]*Department of Engineering – Roma TRE University, Rome, Italy,*
lorenzo.schinaia@uniroma3.it

***Abstract* – The current study is focused on an image segmentation algorithm for Uniformity Quality assessment in Diagnostic Ultrasounds.In particular a mathematical definition of the uniformity in ultrasound images is introducedand a split and merge algorithm performed on sparse matricesto measure uniformity is described. The algorithm is based on the Gray-Level Co-occurrence Matrices and the relativedescriptors,i.e. the Haralick features Entropy, Energy, Maximal CorrelationCoefficientand InformationMeasures of Correlation.Results on2 differentdatasetsof test images with different non-uniformities have been carried on. Several outcomesshow a goodsensitivity and agreement with the mean judgment by 7 human observers, i.e. differences are below 40% in most of the cases.On the basis of previousstudies, the latest developments and results are proposed and commented.**

Keywords – Uniformity measurement, ultrasound, speckle, Gray Level Co-occurrence Matrix, Haralick features

I. INTRODUCTION

Today diagnostic ultrasound (US) systemsarea powerful and widespread technology of medical imaging because of their ability to provide real time images with good resolution and no risks related to ionization radiations.Further advantages are versatility, transportability and costs usually lower than other medical imaging technologies. Since the diagnostic decision is based on the digital image from the ultrasound scanner [1], it can be considered as the starting point of the quality assessment of the whole medical device [2].In literature, among many image quality parameters investigated [2-5],the uniformity is often considered relevant,as in other biomedical fields and technologies [6-8], even if its evaluation seems to be often subjective and not univocal [9], usually performed by specialized technicians without standard criteria: therefore, results are not univocal, depending on testing devices, settings and operator subjectivity [10].Indeed, automatic systems and characterizationprocedures that can support the medical diagnosis are always in developing [11-14]. A recent approach to uniformity objective quantificationapplies pattern recognition and image segmentationto the ultrasound image provided by ultrasound phantoms [15]. In particular,the uniformity into a Region of Interest of the ultrasound image (ROI) is defined as a measure of the diagnostic system capability to display the speckle of a tissue in a homogeneous way within the ROI [15, 16]. From the definition above, the number and dispersion of different textures in the ROI is required to calculate the ROI uniformity index: the higher is the number of textures in the ROI and the differencesamong them, the lower is the ROI uniformity. Several methods in literature studied speckle to either reducing it [17,18] or identifying and characterizingspeckle patterns into the ROI [20, 21]. This isbased on particular sparse matrices, the Gray Level Co-occurrence Matrices (GLCMs) [19], and is characterized by some mathematical operators, the Haralick features. In particular a GLCM is a bi-dimensional histogram where spatial correlations among the grey levels in the ROI are expressed: for all the pixel pairs in the ROI, that are separated by a Inter-Pixel Distance I_{PD} along the orientation θ, the value of the matrix element (p, q) is the number of times that the grey level q occurs after the grey level p. The GLCM is usually normalized by the total number R of paired occurrences, so that from the normalized GLCM $\Phi_{I,\theta}$the texture information is extracted evaluating a set of the Haralick features [19, 20]: for a same I_{PD} and θ , similar textures are characterized by similar sets of values,since the Haralick features are related to different image characteristics, as contrast, brightness, homogeneity and complexity of grey tones spatial distribution, and in the scientific literature there are many examples where they are applied to texture recognition and analysis [19-23]. Nevertheless, althoughtheUS image uniformity quantification can be very useful for both maintenance and research purposes, the application of GLCM and Haralick features extraction to US image quality assessment has not been yet widely applied. To this aim, after a brief overview on main methods and results in literature, some theoretical elements and improvements of the methodin [16] are illustrated and its application to images provided by commercial ultrasound scanners is proposed: measurement results are reported and commented. Future developments are finally discussed.

II. RELATED RESULTS IN THE LITERATURE

Studies on methods for image uniformity objective measurement are quite common in literature, even iftheir application to ultrasound image quality assessment is less investigated, since subjective methods are the mostwidespread [2-3,9]. InHangiandreou*et al.* [24, 25] in-air images and speckle images of a uniform region of a ultrasound phantom are visually inspected: vertical dark bands (axial hypoechoic artifacts) usually indicate a localized transmission/reception failure. On the other hand,in Martensson*et al.* [26] a probe tester is proposed for the relative sensitivity measurement of each piezoelectric element of the ultrasound probe: defective channels were found by means of the objective evaluation of the local sensitivity. Another computer based method is reported in [27-29], where the uniformity of the echosignal or noise is evaluated by imaging a uniform region of aultrasound tissue mimicking phantom and.an in-air-image respectively:the averaged signal pixel values at a given depth are plotted as a function of the scanning direction and a local decrease of a few dB or more may indicate system failures. In [15], the image gray level histogram of the ROI is weighted by sigmoid functions to determine the spread of the image histogram due to non-uniformities. Anyway, all the above approaches have been based on a first order statistic of pixel values into the ROI, while in [16] the correlation between pixels is used to determine the speckle pattern characteristics and homogeneity to quantify the ultrasound image uniformity: this approach is described in detail in the following sections.

III. DESCRIPTION OF THE METHOD

In the first two sections A and B of this paragraph the definition of the ultrasound image uniformity and the input variables criterion are reported. The third section C examines the block-diagram of the algorithm proposed. Finally, the last paragraph D explains the datasets used.

A. Uniformity: definition

The definition of image uniformity is based on the principle thatit is possible to define a segmentation criterion todivide the image into areas that are characterized by features that differ significantly from those of the adjacent neighbors: two adjacent areas with similar (or equal) features are considered uniform (therefore both of them belong to the same area). Sometimes segmentation is made easier when it follows some foreground extraction technique [30]. The image uniformity is measured from the number of ROI partitions and the quantification of their difference after the segmentation process (split & merge algorithm), to this aima set of features (Haralick features)are evaluated over the whole image and its partitions. Therefore, a preliminary choice of theimagefeatures should be done, since the segmentation process into regions depends on thechosen features. In [8] the image uniformity is defined as:

$$U_{ROI} = 1 - \Gamma_{ROI} \tag{1}$$

the non-Uniformity index Γ_{ROI} in (1) depends on the image features. The dispersion (i.e. standard deviation) of the sub-ROIs characteristics at the end of the segmentation process is used to measure the ROI uniformity $U_{ROI,I_{PD},\{f_1..f_k\}}$[31], as each sub-ROI corresponds to a specific set of several GLCM feature values f_k as well as textures:

$$U_{ROI,I_{PD},\{f_1\cdots f_k\}} = \left(1 - \frac{\sigma_{\{f_1\cdots f_k\}}}{\psi}\right)\cdot 100 \tag{2}$$

Where $\sigma_{\{f_1..f_k\}}$ is the standard deviation of $\{f_1 .. f_K\}$ among all sub-ROIs and ψ a normalization coefficient, adapted from [31]. In the algorithm developed the $U_{ROI,I_{PD},\{f_1..f_k\}}$can beevaluated for more inter-pixel distances I_{PD}: in that case the finalvalue of the image uniformity U_{ROI}isassociated to the minimum of the$U_{ROI,I_{PD},\{f_1..f_k\}}$. For a same ROI, numerical results mainly depend on (a) orientationsand (b) distance I_{PD}in GLCM calculation,(c) the GLCM features f_k, , (d) ROI size and position (e) threshold values (split and merge) for f_k discrimination between not homogeneous sub-ROIs [16].

B. Setting Input variables

The most important input variables here considered are: (1) features type, GLCM (2) directions and (3) inter-pixel distances I_{PD}, (4) the threshold values of the differences between features of adjacent sub-ROIs for the segmentation criterion, i.e.differences above the thresholds are associated to sub-ROIs of different textures.

From other studies performed by the authors the following Haralick features have been selected: *Entropy (f_1), Energy (f_2), Maximal Correlation Coefficient (f_3), Information Measures of Correlation II (f_4).*Everyfeature above is evaluated on GLCMs obtained for the two directions, θ= 0° and θ= 90°, at a specific inter-pixel distance I_{PD}.With this aim a Fast Fourier Transform (FFT) analysis on each test image has been implemented for both directions to determine the I_{DP} from the frequency of the first peaks detected in the corresponding FFT spectrums by means of an adaptive threshold algorithm: in order to reduce computational complexity, only one I_{DP} value is here selected for each direction in the test image. In particular the adaptive threshold algorithm finds the first

FFT peak in a spatial frequency interval where the minimum is related to the ROI size and the maximum is dependent on both the ultrasound scanner spatial resolution and the operator visual acuity.On the other hand, the optimal threshold values for the segmentation criterion (split and merge algorithm) have been estimated for each feature on a speckle test image, assumed as uniform and evaluating the U_{ROI} at different threshold levels (range between 0 and 1): for each feature the optimal threshold is determined in correspondence of the maximum uniformity U_{ROI}.

C. Block-Diagram of the sparse matrix algorithm

In this section, the block diagram of the method proposed is described (fig.1). The code has been implemented in a MatLab environment (Matworks 2014), with functions based on the use of sparse matrices. In particular, the image (ROI) is portioned into areas (sub-ROIs) that are characterized by different sets $\{f_1, f_2, f_3, f_4\}$, corresponding to different textures. More specifically a ROI is iteratively decomposed into 4 quadrants (sub-ROIs) on the basis of the difference among the values of the four features above (fig.2). The decomposition carries oniteratively foreach sub-ROI until either the above differences are all below a threshold value (2nd condition of the block diagram: *Predicate Function and Threshold Parameter*) or the sub-ROI size is equal to 2ℓ, where ℓ is the side of the smallest square area resolvable by the diagnostic system (1st condition of the block diagram: *Step Dimension*).

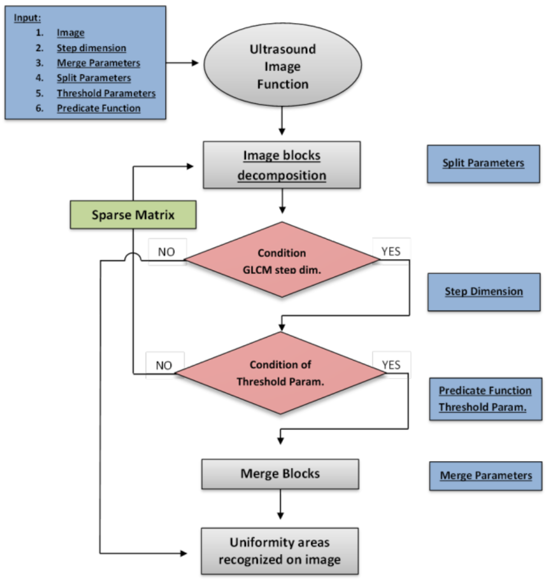

Fig. 1. Block diagramof the sparse matrix algorithm.

The GLCM features are compared between ROI quadrants on the six directions showed in Figure 2. Finally, depending on the Haralick features that have been considered for the merge operation, the sparse matrix obtained is solved to get the final decomposition: the corresponding image is subdivided into several areas of different uniformity values (Fig.3).

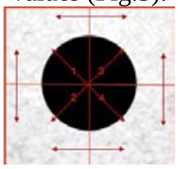

Fig. 2. Example of the directions taken into account for the comparison between features in the four quadrants, i.e. along horizontal, vertical and diagonal orientations.

In order to give a visual example of segmentation operation applied by the algorithm, in the following figure 3 two images, and their segmentation areas, are shown.

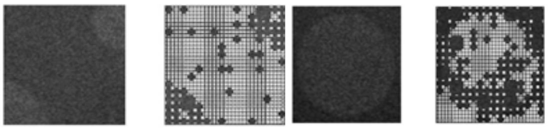

(a) (b)

Fig. 3. Examplesof outcomes of the segmentation procedure. (a) three and (b) two areas with different speckle pattern.

D. Dataset used for Uniformity algorithm tests

In this study, three datasets are used for testing the proposed method: 1) synthetics images, 2) real images from a same ultrasound scannerat different compression and gain settings, 3) real images from different commercial diagnostic systems and affected by different non-uniformities. The synthetic images (Circles Image Test Set or CITS) are of 128x128 pixelsize and produced by theMatLab 2014 software.In particular,sixclasses of images with circles at differentsize (i.e. 2, 4, 6, 16, 18 and 30 pixel radius respectively) and speckle noise level have been tested (figure 4), ascircles can be associated todifferent non uniformities in medicalpractice (e.g. hepatoma - hepatocellular carcinoma).

A second image dataset contains vertical black band (Stripes Image Test Set or SITS), as they can be associated to non uniformities due to broken piezoelectric elements in the ultrasound probes. The images are collected at different Compression settings (i.e. 30, 45 and 60) and Gain level (i.e. range 50%-100% in steps of 5%) by means of a Philips iE33 ultrasoundsystem, equipped with a phased array probe, i.e. Philips S8-3, that has been applied to a*CIRS model 047* ultrasound phantom (fig. 5) .

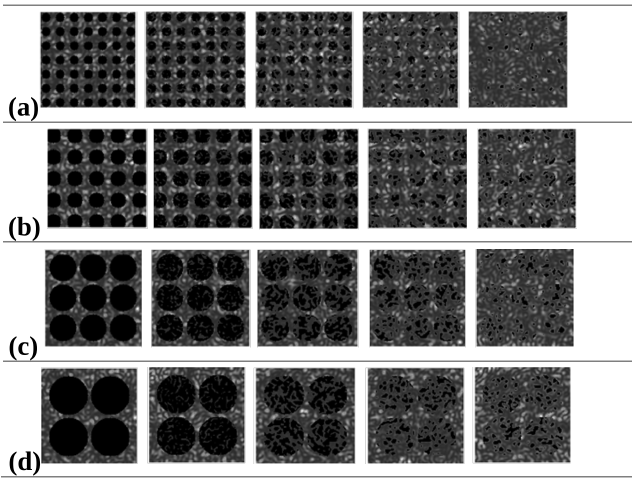

Fig. 4. Synthetic image dataset (circles dataset or CTS). Example of test images with circles of different size and speckle noise level (increasing from left to right). (a) 2px radius (b) 6px radius (c) 18px radius (d) 30 pixel radius

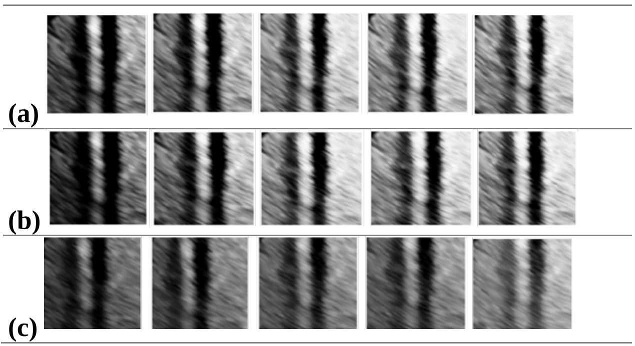

Fig. 5. Example of the 128px×128px test images from the second dataset at different compression settings and gain level (SITS). (a) Compression settings 30 (maximum compression), (b) Compression settings 45 and (c) Compression settings 60 (minimum compression). Gain level ranges from 50% (1st column on the left) to 100%.

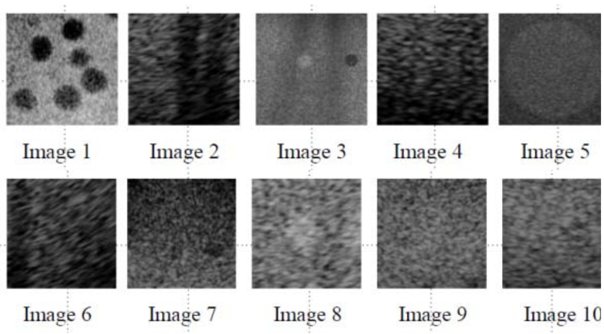

Fig. 6. Uniformity Image Test Set (UITS).

In figure 5 test images are of the same size, i.e.128px×128px, and collected at the same transmit power (i.e. maximum), position and field of view (i.e. 13 cm) in the ultrasound image. Finally, the algorithm performances have been tested on a set of ultrasound images (Uniformity Image Test Set or UITS) acquired from different commercial diagnostic systems and affected by different non-uniformities (Fig. 6).

IV. RESULTS AND DISCUSSIONS

On theCITS the software recognition capability has been tested depending onthe non-uniformities size, number and speckle noise level: in table 1 the corresponding uniformity values are reported.

Table 1. Uniformity values (%) for thesynthetic image dataset (CITS) at different Speckle Noise Level.Relative uncertainties of the methodranges up to 28%

Circle radius size(px)	Speckle Noiselev.1	Speckle Noise lev.2	Speckle Noise lev.3	Speckle Noise lev.4	Speckle Noise lev.5
r = 2	1	1	2	36	75
r = 4	1	1	5	61	75
r = 6	2	3	58	61	75
r = 16	1	7	16	61	88
r = 18	3	3	54	58	75
r = 30	3	22	35	65	65

In particularfor low speckle noises within the objects (Level 1, 2 and 3), the method provided low values of Uniformity, likely due to the detection of non uniformity areas into the image. On the other hand,the uniformity values increase with the speckle noise level and the size of not-uniformities. In order to considerthe method outcomesdepending on Compression and Gain settings, results for SITS are evaluated and shown in table 2.

Table 2. Uniformity values (%) at different compression and gain settings. Relative uncertainties of the method ranges up to 28%

Gain	**Comp**.settings 30	Comp.settings 45	Comp.settings 60
55%	34	54	34
60%	38	58	46
65%	46	60	52
70%	57	62	55
75%	54	62	62
80%	60	61	61
85%	61	65	60
90%	58	59	62
95%	62	61	60
100%	58	60	61

In particular, no significant differences have been found depending on the compression:all differences are below 12% (they are below 4% in most cases), that is less than the estimated uncertainty of the method, i.e. 28%. Anyway, the outcomes seem reasonable as the black bands are clearly visible in all test images and the segmentation follow the band geometry also in the worst cases, where the images are almost black because of the low gain settings (figure 7).

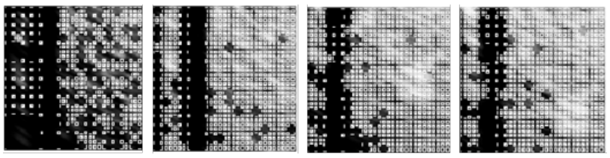

Fig. 7. Example of areas segmentation of black bands image.

Table 3. Uniformity values: Algorithm$U_A$compared with Human responseU_H(Tests for Visual Uniformity assessment). Relative uncertainties of the U_A ranges up to 28%

UITS	U_A(%)	U_H (%)
Image 1	1	11 ± 6
Image 2	38	24± 11
Image 3	46	39 ± 16
Image 4	65	47± 7
Image 5	27	50± 25
Image 6	58	50 ± 8
Image 7	62	59 ± 15
Image 8	82	65 ± 8
Image 9	53	88± 18
Image 10	75	89 ± 7

In table 3, for most of the images in fig. 7the algorithm outcomes$U_A$suggest a good agreement with the mean judgment U_H expressed by 7 human observers on the UITS, i.e. most of the differences between uniformity values are below 40% referred to the human judgment, half of them is below 30% , while U_A relative uncertainties have been estimated to range up to 28%[9].Nevertheless, some differences can be significant: since the uniformity values are derived from considering all the features, it is reasonable that some of them have predominant behavior and decrease (or increase) the value of the uniformity measurement U_{ROI} also for images where patterns may be considered more (or less) homogenous by the human observers, i.e. max correlation. On the other hand, differences between U_A and $U_H$are likely due also to the unexperienced judgement of the observers engaged in the test, as it can be confirmed by the high uncertainties of U_H.

V. CONCLUSIONS

In this work, an image segmentation method for Uniformity Quality assessmentin diagnostic ultrasound is reported with some results.Most of the algorithm outcomes are in agreement with the judgment of 7 human observers on an image test set from commercial ultrasound scanners but, despite the encouraging outcomes (most of the differences are below 40%), further work is required to improve the method, its robustness and characterization. In particular,more tests should be done, also with different reference images, to better estimate the uncertainty of the methoddepending on the numerous variables (orientations and inter-pixel distances in GLCM calculation, discrimination thresholds, ROI characteristics,)and toprovide a robust reference scale based on the judgment of experienced observers. Moreover, an in-depth study on algorithm sensitivity to non-uniformities and its relationship with the Haralick features should be conducted.

REFERENCES

[1] Chow, Li Sze, and Raveendran Paramesran. *Review of medical image quality assessment*. Biomedical Signal Processing and Control 27 (2016): 145-154.

[2] W.R. Hedrick, D. L. Hykes, D. E. Starchman, *Ultrasound Physics and instrumentation*, Elsevier Mosby, 2004

[3] Andrea Scorza, Francesco Orsini, Salvatore Andrea Sciuto (2017), *Use of phantoms and test objects for Local Dynamic Range evaluation in medical ultrasounds: a preliminary study*, In: 2017 IEEE International Instrumentation and Measurement Technology Conference (I2MTC 2017) Proceedings, Torino, Italy, 2017, pp. 1094-1099

[4] Marinozzi, F., Bini, F., D'Orazio, A., Scorza, A.,*Performance tests of sonographic instruments for the measure of flow speed* (2008) IST 2008 - IEEE Workshop on Imaging Systems and Techniques Proceedings, art. no. 4659939, pp. 50-55.

[5] Scorza, A., Lupi, G., Sciuto, S.A., Bini, F., Marinozzi, F.*A novel approach to a phantom based method for maximum depth of penetration measurement in diagnostic ultrasound: A preliminary study*(2015) 2015 IEEE International Symposium on Medical Measurements and Applications, MeMeA 2015 - Proceedings, art. no. 7145230, pp. 369-374..

[6] C. De Marchis, M. Schmid, D. Bibbo, I. Bernabucci, S. Conforto, *Inter-individual variability of forces and modular muscle coordination in cycling: A study on untrained subjects* Human Movement Science, 32 (6), pp. 1480-1494, 2013.

[7] S. Comani, L. Velluto, L. Schinaia, G. Cerroni, A. Serio, S. Buzzelli, S. Sorbi, B. Guarnieri, *Monitoring neuro-motor recovery from stroke with high-resolution EEG, robotics and virtual reality: a proof of concept*. IEEE Transactions on Neural System and Rehabilitation Engineering, 2015 Apr 22.

[8] E. Filho, M. Bertollo, G. Tamburro, L. Schinaia, J. Chatel-Goldman, S. Di Fronso, C. Robazza, S. Comani, *Hyperbrain features of team mental models within a*

juggling paradigm: a proof of conceptPeerJ: Summer 2016;

[9] E. L. Madsen, B. S. Garra, J. A. Parks, A. C. Skelly, and J. A. Zagzebski, *AIUM Quality Assurance Manual for Gray-Scale Ultrasound Scanners (Stage 2)*, American Institute of Ultrasound in Medicine, Laurel, MD, 1995.

[10] Scorza A., Conforto S., Sciuto S.A. (2015). *A comparative study on the influence of probe placement on quality assurance measurements in B-mode Ultrasound by means of ultrasound phantoms*, The Open Biomedical Engineering Journal, 9:164-78.

[11] Carmen D'Anna, Silvio Scena, Andrea Scorza, Maurizio Schmid, Francesco Orsini, Salvatore Andrea Sciuto, Silvia Conforto (2017) *A preliminary study on the validation of an automatic measurement method for Functional Reach assessment by stereophotogrammetry*, In: 2017 IEEE International Instrumentation and Measurement Technology Conference (I2MTC 2017) Proceedings, Torino, Italy, 2017, pp. 962-966.

[12] Francesco Orsini, Andrea Rossi, Andrea Scorza, Salvatore Andrea Sciuto (2017), *Development and preliminary characterization of a novel system for the force platforms dynamic calibration*, In: 2017 IEEE International Instrumentation and Measurement Technology Conference (I2MTC 2017) Proceedings, Torino, Italy, 2017, pp. 1082-1087

[13] Francesco Orsini, Andrea Scorza, Andrea Rossi, Fabio Botta, Salvatore Andrea Sciuto, Riccardo di Giminiani (2016). *A preliminary uncertainty analysis of acceleration and displacement measurements on a novel WBV platform for biologic response studies*. In: 2016 IEEE International Symposium on Medical Measurements and Applications (MEMEA 2016) Proceedings, Benevento, Italy, 2016, pp.137-142

[14] Andrea Rossi, Francesco Orsini, Andrea Scorza, Fabio Botta, Salvatore Andrea Sciuto, Riccardo di Giminiani (2016). *A preliminary characterization of a Whole Body Vibration platform prototype for medical and rehabilitation application* In: 2016 IEEE International Symposium on Medical Measurements and Applications (MEMEA 2016) Proceedings, Benevento, Italy, 2016, pp.131-13

[15] A. Scorza, G. Lupi, S. A. Sciuto, L. Battista, J. Galo, *A preliminary study on a method for objective uniformity assessment in diagnostic ultrasound imaging.* In: 2015 IEEE International Instrumentation and Measurement Technology Conference (I2MTC 2015) Proc, Pisa, Italy, pp. 1628-1633, 2015

[16] A. Scorza, S. Conforto, G. Lupi and S. A. Sciuto, *A texture analysis approach for objective uniformity evaluation in diagnostic ultrasound imaging: a preliminary study*, In: 37th Annual International Conference of the IEEE Engineering in Medicine and Biology Society (EMBC 2015) Proc, Milano, Italy, pp. 6317-6320, 2015.

[17] S. Adabi, E. Rashedi, S. Conforto, D. Mehregan, Q. Xu, M. Nasiriavanaki, *Speckle reduction of OCT images using an adaptive cluster-based filtering*, Progress in Biomedical Optics and Imaging - Proceedings of SPIE, 10053, art. no. 100532X, 2017

[18] S. Adabi, S. Conforto, A. Clayton, AG Podoleanu, A. Hojjat, MRN Avanaki. *An intelligent speckle reduction algorithm for optical coherence tomography images*, PHOTOPTICS 2016 - Proceedings of the 4th International Conference on Photonics, Optics and Laser Technology, 40-45. 2016

[19] R.M. Haralick, K. Shangmugam, I. Dinstein, *Textural features for image classification*, IEEE Trans. Syst. Man Cybern. SMC-3 (6) (1973) 610–621.

[20] MH Soomro, G Giunta, A Laghi, D Caruso, M Ciolina, C De Marchis, S Conforto, M Schmid, *Haralick's texture analysis applied to colorectal T2-weighted MRI: A preliminary study of significance for cancer evolution*, Proceedings of the 13th IASTED International Conference on Biomedical Engineering, BioMed 2017, art. no. 7893262, pp. 16-19, 2017

[21] R. M. Haralick,*Statistical and structural approaches to texture*, Proc. IEEE 67, 786-804, 1979

[22] S. Mukherjee, A Chakravorty, K. Ghosh, M. Roy1, A. Adhikari and S. Mazumdar, *Corroborating the subjective classification of ultrasound images of normal and fatty human livers by the radiologist through texture analysis and SOM*" IEEE, *15th International Conference on Advanced Computing and Communications*, 2007

[23] M. H. Soomro et al., *Haralick's texture analysis applied to colorectal T2-weighted MRI: A preliminary study of significance for cancer evolution* , 13th IASTED International Conference on Biomedical Engineering (BioMed), Innsbruck, Austria, 2017, pp. 16-19.

[24] N. J. Hangiandreou, S. F. Stekel, D. J. Tradup, K. R. Gorny, D. M. King, *Four-year experience with a clinical ultrasound Quality Control program,Ultrasound Med. Biol.*, vol. 37, no. 8, pp. 1350–1357, 2011.

[25] N. Hangiandreou, *Ultrasound Quality Control: A Practical Overview of Tests, Methods, and ACRAccreditation Requirements*, AAPM Annual Meeting, 2013

[26] M. Martensson, M. Olsson, B. Segall, A. G. Fraser, R. Winter, L. A. Brodin, *High incidence of defective ultrasound transducers in use in routine clinical practice*, Eur. J. Echocardiogr., vol. 10, no. 3, pp. 389–394, 2009.

[27] C. Kollmann, C. deKorte, N. J. Dudley, N. Gritzmann, K. Martin, D. H. Evans; EFSUMB Technical Quality Assurance Group--US-TQA/B. *Guideline for Technical Quality Assurance (TQA) of ultrasound devices (B-Mode)--version 1.0 (July 2012): EFSUMB Technical Quality Assurance Group--US-TQA/B*, Ultraschall Med., vol. 33, no. 6, pp. 544-549, Dec. 2012.

[28] International Electrotechnical Commission (IEC). *IEC 62736 Ed. 1.0 Quality Control of Diagnostic Medical Ultrasound Systems*. Draft Geneva. 2011.

[29] E. Sassaroli, A. Scorza, C. Crake, S. A. Sciuto and M. A. Park, *Breast Ultrasound Technology and Performance Evaluation of Ultrasound Equipment: B-Mode*, in IEEE Transactions on Ultrasonics, Ferroelectrics, and Frequency Control, vol. 64, no. 1, pp. 192-205, Jan. 2017. doi: 10.1109/TUFFC.2016.2619622

[30] S. Conforto, M. Schmid, A. Neri, T. D'Alessio, *A neural approach to extract foreground information from human movement images*, Comput Methods Programs Biomed, 82(1):73-80, 2006.

[31] M. D. Levine, A. M. Nazif, *Dynamic Measurement of Computer Generated Image Segmentations,IEEE Trans. On Pattern Analysis and Machine Intelligence*, vol. PAM1-7, n°2, 155-, 1985.